ELSEVIER

Polymer 43 (2002) 681–691

polymer

www.elsevier.com/locate/polymer

Study of ionic conductivity and microstructure of a cross-linked polyurethane acrylate electrolyte

M. Digar, S.L. Hung, H.L. Wang, T.C. Wen*, A. Gopalan[1]

Department of Chemical Engineering, National Cheng Kung University, Tainan 701, Taiwan, ROC

Received 23 July 2001; received in revised form 17 September 2001; accepted 28 September 2001

Abstract

A cross-linked polyurethane acrylate (PUA) was synthesized by end capping 4,4′-methylene bis(cyclohexyl isocyanate), H_{12}MDI/poly-(ethylene glycol), PEG based prepolymer with hydroxy ethyl acrylate (HEA). Significant interactions of the Li^+ ions with the soft and hard segments of the host polymer have been observed for the PUA complexed with lithium perchlorate ($LiClO_4$) by means of differential scanning calorimetry (DSC), Fourier transform infra-red (FTIR) spectroscopy, ^{7}Li magic angle spinning (MAS) NMR measurements and thermogravimetric analysis (TGA). The ^{7}Li MAS NMR investigation of the PUA indicates the presence of at least three distinct Li^+ sites at lower temperature, which merge to a single one at higher temperature in similar line with uncross-linked polyurethane. The results of TGA, DSC and FTIR spectroscopy support the formation of different types of complexes by the interaction of the Li^+ ions with different coordination sites of PUA. No detectable interactions could be observed between Li^+ ions and groups in HEA. The DSC data indicates the formation of transient cross-links with the ether oxygens of the soft segment and mixing of soft and hard phases induced by the Li^+ ions. In addition, a Vogel–Tamman–Fulcher (VTF) like temperature dependence of ionic conductivity implies coupling of the ion movement with the segmental motion of the polymer chains in the cross-linked environment. Predominant formation of contact ion pairs of $LiClO_4$ has been consistently observed through AC conductivity, DSC and NMR spectroscopic results. Swelling measurements of PUA with plasticizers reveal the improved dimensional stability for these cross-linked PUA in comparison with uncross-linked polyurethane.

Keywords: Ionic conductivity; Polyurethane acrylate electrolyte; Differential scanning calorimetry

1. Introduction

For the last few years, polymer solid electrolytes based on polyether matrices have attracted considerable attention [1–3] mainly due to the possibility of their application in various electrochemical devices such as alkali metal batteries, electro chromic displays and sensors, and fuel cells working at ambient and moderate temperatures. It has been found that the mobility of the ions is coupled with the segmental motion of the polymer chains, and hence the presence of a flexible, amorphous phase is essential for high conductivity in polymeric electrolytes [4,5]. Several attempts have been made to obtain amorphous polyether matrices, which exhibit high ionic conductivity over a wide temperature range [2,3]. Polyethylene oxide (PEO) is the reference polymer for ionic conduction, since it is the best host matrix for inorganic salts. It has been found that the comb-branched polymers based on the phosphazene backbone and having oligomeric PEO in the side chain are amorphous in nature and hence one of the highest conductive conventional polymer electrolyte [6,7]. The dimensional stability and mechanical properties were however improved by cross-linking with poly(ethylene glycol) (PEG) [8] or by irradiation with γ-rays [9].

Besides PEO, several alternative systems, like poly-(methyl methacrylate) (PMMA), polyacrylonitrile (PAN), poly(vinylidine fluoride) (PVdF), poly(vinyl chloride) (PVC), etc. have been investigated including the thermo-plastic polyurethane (TPU) [10–25]. In polyurethane, the condensation of a diisocyanate with a polyether macro monomer leads to the formation of a segmented polymer having a general structure $(A–B)_n$, where B is the soft segment usually formed from one or more of polyether or polyester polyol and A is the hard segment formed by extending a diisocyanate with low molecular weight diol or diamine. The TPUs are characterized by a unique

* Corresponding author. Tel.: +886-6-2385-487; fax: +886-6-2344-496.
E-mail addresses: tcwen@mail.ncku.edu.tw (T.C. Wen), algopal_99@yahoo.com (A. Gopalan).
[1] Address: Department of Industrial Chemistry, Alagappa University, Karaikudi 630 003, India.

0032-3861/02/$ - see front matter
PII: S0032-3861(01)00655-3

two-phase microstructure where the hard segment domains are distributed in a soft segment matrix [23]. The primary driving force for phase separation or domain formation is the strong intermolecular interactions of the urethane units, which are capable of forming interurethane hydrogen bonds. The rubbery soft segments can dissolve alkali metal salts without formation of ionic clusters, which may be due to the interaction of the ether oxygens with the alkali metal ions [22,23]. Furthermore, the low glass transition temperature (T_g) and hence higher segmental motion of these polyethers lead to higher mobility of the dissolved ions. The ability to dissolve alkali metal ions along with higher ionic mobility results in a relatively high ionic conductivity of the electrolytes. The hard segment domains, which are in the glassy state and either distributed or interconnected throughout the rubbery phase of the soft segment, act as reinforcing filler and hence contribute to the dimensional stability of the polymer electrolytes.

The interest in using TPU as matrix for polymer electrolyte is related to the possibility of increasing the mechanical strength of linear polyethers due to the phase separated microstructure of TPU. Poly(ethylene glycol) (PEG), poly(propylene glycol) (PPG) and poly(tetramethylene glycol) (PTMG) are the three main polyether polyols that are used as soft segments in TPU based electrolytes [10–22]. Watanabe et al. [13,14] investigated the morphology and ionic conductivity of a 4,4′-methylene bis(phenyl isocyanate)/poly(propylene glycol)/ethylene diamine based TPU electrolyte doped with $LiClO_4$. This system exhibited low conductivity ($\sim 10^{-8}$ S cm^{-1} at 40°C), and the conductivity isotherms did not show a pronounced dependence on salt concentration. McLennaghan et al. [11,12] have studied a TPU based on 4,4′-methylene bis(phenyl isocyanate)/poly(ethylene glycol)/1,4-butanediol having a range of hard segment concentration (22–76%). They observed that the best performance is achieved by the phase-separated nature of TPU with the lowest hard segment concentration. They concluded that the ionic conductivity is sensitive to the phase separated nature of TPU and a lower T_g of the soft segment leads to higher conductivity. Seki et al. [16] studied a 4,4′-methylene bis(phenyl isocyanate)/poly(tetramethylene glycol)/1,4-butanediol based commercial TPU having different hard segment concentration. In addition to an increase in conductivity with salt concentration, they observed a decrease in overall bulk conductivity with increase in hard segment concentration. van Heuman et al. [15] reported a change in morphology of a 4,4′-methylene bis(phenyl isocyanate)/poly(tetramethylene glycol)/1,4-butanediol based TPU as a function of salt concentration. As a result of the change in morphology due to the complexation with Li-salts, the thermal stability of the system is improved over the undoped TPU. Forsyth et al. [17] reported the effect of plasticizer addition on the ionic structure and mobility in a sodium triflate doped TPU based solid polymer electrolyte by using ^{23}Na and ^{19}F NMR spectroscopy. Addition of plasticizers results in an upfield chemical shift for the ^{23}Na resonance as a consequence, of a decreased ion association and an increased cation plasticizer interaction. Ferry et al. [18] carried out a spectroscopic investigation of a commercial TPU complexed with $LiClO_4$. Their results suggest a competition between the H-bond and Li^+ ions coordination, especially in the hard segments of the host polymer. Ng et al. [19] investigated a urethane cross-linked PEG polymer doped with $LiClO_4$ and $LiCF_3SO_3$ by dynamic mechanical thermal analysis (DMTA) and solid state NMR measurements, and indicated from their ^{7}Li spin lattice relaxation time (T_1) measurements that the cationic environment was similar regardless of the nature of the anion. A shift in the mechanism of the ion mobility has been suggested where Li^+ ions are transported between aggregates and hence is less influenced by the segmental motion of the polymer chain. In our earlier publications [21,22], a 4,4′-methylene bis(cyclohexyl isocyanate)/poly(ethylene glycol)/ethylene diamine based TPU system has been investigated in detail by ^{7}Li and ^{13}C solid-state NMR, DSC, FTIR and AC impedance measurements. At least two distinct Li^+ sites have been identified in the $LiClO_4$ doped TPU by measuring the ^{7}Li NMR spectrum under conditions of magic angle spinning (MAS) and high power proton decoupling [21].

It has been found that the polymer electrolytes based on host polymer matrices incorporating oxyethylene chains ($-CH_2-CH_2-O-$) yield the highest ionic conductivity. Hence, the PEG based TPU shows highest conductivity compared to PPG and PTMG based TPUs. The higher conductivity of PEG based systems is due to the optimum spacing and conformational flexibility provided by the PEO units. This is supported by the fact that poly(methylene oxide) ($-CH_2O-$) and poly(trimethylene oxide) ($-CH_2-CH_2CH_2-O-$) do not act as solvent for ions [26]. Although the conductivity of the PEG based TPU electrolyte is among the highest, its mechanical strength and stability towards commercial liquid electrolytes are among the poorest.

Through careful analysis of literature, it becomes clear that TPU type polymer electrolytes with $-(CH_2-CH_2-O)-$ units in it can show better conductivity in comparison with the other analogs. However, the dimensional stability of the electrolyte must be improved to have practical viability. Keeping this in view, in the present study, we have specifically cross-linked polyurethane containing $-(CH_2-CH_2-O)-$ units by interacting the end groups of PU prepolymer with hydroxy ethyl acrylate (HEA). A cross-linked polyurethane acrylate (PUA) was hence synthesized by end capping a 4,4′-methylene bis(cyclohexyl isocyanate) (H_{12}MDI)/poly(ethylene glycol) (PEG) based prepolymer with HEA followed by thermal cross linking. Systematic characterization studies of the cross-linked PUA in the presence of $LiClO_4$ were made with differential scanning calorimetry (DSC), Fourier transform infra-red (FTIR) spectroscopy, ^{7}Li solid state NMR measurements and AC impedance measurements to bring out the phase transitions, interaction of Li^+ ions with segments of PUA and

conductivity in the cross-linked environment of PU. Dimensional stability of the cross-linked PUA was also tested by swelling measurements with plasticizers. Detailed discussion of the results reveal that the synthesized PUA can have improved dimensional stability without significant loss of conductivity.

2. Experimental details

2.1. Materials

Poly(ethylene glycol) (PEG; $M_w = 2000$; Showa) was dehydrated under reduced pressure at 80°C for 24 h before use. 4,4′-methylene bis(cyclohexyl isocyanate) (H_{12}MDI) and HEA (both Aldrich) were used as received. $LiClO_4$ (Aldrich) was dehydrated at 120°C under reduced pressure for 72 h. Two commercial battery electrolytes LP-20 and LP-30 (Merck) were used as received. These two electrolytes are 1 M solutions of $LiPF_6$ in propylene carbonate/diethyl carbonate (PC/DEC) and ethylene carbonate/dimethyl carbonate (EC/DMC), respectively. All other reagents and chemicals were used without further purification.

2.2. Synthesis of PUA

The PUA was synthesized by a two-step addition process, where the prepolymer was made by the reaction of excess of H_{12}MDI with PEG-2000 and then capping the end NCO groups by the reaction with HEA. The prepolymer was made by allowing the mixture of H_{12}MDI and PEG-2000 to react at 85°C for 6 h with constant stirring under a dry nitrogen blanket. After the prepolymer formation was over (confirmed by estimation of NCO groups by di-butyl amine back titration method), dimethyl formamide (DMF) was added to dissolve the prepolymer. The temperature of the mass was reduced to 60°C and then required amount of HEA was slowly added to the reaction mixture. The reaction was allowed to continue for 2 h and then it was terminated by the addition of ~0.2 g of methanol. The molar ratio of H_{12}MDI, PEG and HEA, maintained for this PUA, was 2:1:2. The structure of the synthesized PUA is shown in Fig. 1.

2.3. Preparation of the polymer electrolytes

Solid polymer electrolytes (SPE) were prepared by mixing various concentration of $LiClO_4$ in DMF with the PUA solution in DMF. 2,2′-azobisisobutyro nitrile (AIBN) was also mixed with the PUA for thermal cross-linking through the acrylate end groups. After homogeneous mixing, the solution was cast into Teflon plates. Solvent removal and simultaneous cross-linking were done at 80°C under reduced pressure for 72 h. The films were then kept inside an argon filled glove box for several days before further experiments. The undoped film was also made in the same way but having no $LiClO_4$ for swelling study in liquid electrolytes.

2.4. Thermogravimetric analysis

TGA experiments were performed using a Perkin Elmer TGA 7/DX Thermal Analyser with a scan rate of 20°C/min until 650°C under nitrogen atmosphere.

2.5. Differential scanning calorimetry

DSC experiments were carried out using a DSC 2010 Differential Scanning Calorimeter (TA Instruments, USA) over a temperature range −120–150°C at a scan rate of 10°C/min. The dry samples were sealed in Al crucibles inside the glove box. The sealed samples were taken out of the glove box only at the time of DSC experiments. The samples were first annealed at 150°C for 10 min, cooled down to −120°C and then scanned. All the thermograms are base line corrected and calibrated against Indium metal. Glass transition temperature (T_g) was reported as the midpoint of the transition process and melting temperature was the peak temperature.

2.6. Fourier transform infra-red spectroscopy

FTIR spectra were taken at ambient temperature using a Nicolet 550 equipment with a wave number resolution of 2 cm^{-1}. Sample for FTIR was made by casting the polymer–salt-initiator mixture directly on KBr pellets and then simultaneously dried and cross-linked at 120°C for 48 h. One hundred and twenty-eight scans were signal averaged to increase the *s/n* ratio.

2.7. Solid state NMR experiments

^{7}Li MAS NMR spectra were recorded with a Bruker AVANCE-400 NMR spectrometer, equipped with a 7 mm double resonance probe, operating at 400.13 MHz for ^{1}H and 155.5 MHz for ^{7}Li. Typical NMR experimental conditions were as follows: $\pi/2$ duration, 3 μs; recycle delay, 2 s; ^{1}H decoupling power, 65 kHz and spinning speed, 3 kHz. Chemical shifts were externally referenced to solid LiCl at 0.0 ppm.

2.8. AC impedence measurements

Impedance measurements of the polymer electrolytes were performed using thin films made by casting from solution and subsequent cross-linking and drying (as described earlier). Film thickness was maintained in the range of 200–250 μm and the area of contact was 0.785 cm^2. For measurement of ionic conductivity, the samples were sandwiched between two stainless steel electrodes. The electrodes were then fixed in an airtight double wall glass cell, through the outer jacket of which thermostated water was circulated for measurements at different temperatures. Cell assembly was carried out in dry argon atmosphere

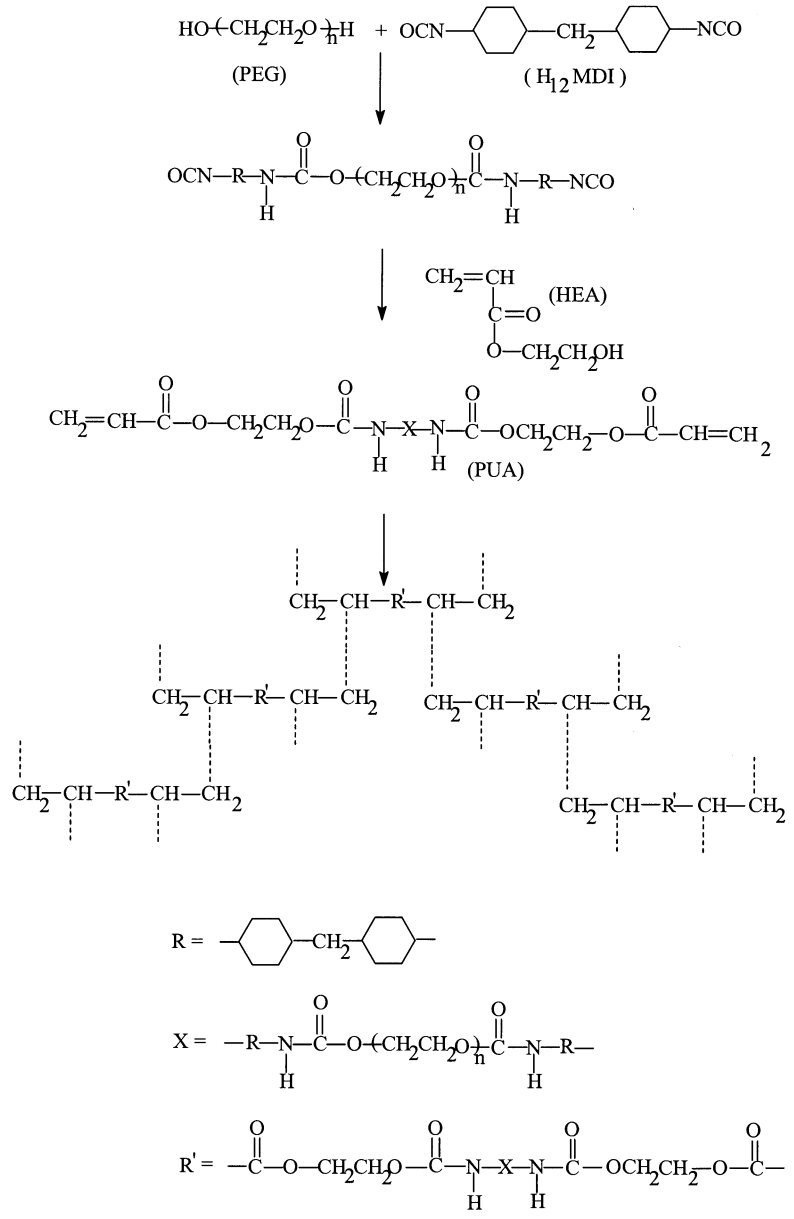

Fig. 1. Schematic representation of the synthesis of PUA.

inside a glove box (Vacuum Atmosphere Company, USA). Conductivity measurements were performed using the Autolab with PGSTAT 30 (Eco Chemie B. V., Netherlands) controlled by the Frequency Response Analysis system software under an oscillation potential of 10 mV.

2.9. Swelling study

Swelling experiments of PUA was carried out inside the glove box by dipping a preweighed film (~500 mg) in the two liquid electrolytes. The films were kept immersed for different time periods after which the films were withdrawn, the surface electrolytes were removed by soaking with a filter paper and then reweighed. Percent swelling (S_w) is expressed as

$$S_w = 100(w - w_0)/w_0 \quad (1)$$

where w_0 is the initial weight of the film and w is the weight of the film after swelling.

3. Results and discussion

The cross-linked PUA made from H_{12}MDI, PEG (M_w = 2000) and HEA was found to show phase transitions different from the uncross-linked TPU in the presence of $LiClO_4$. However, the glass transition temperature of the soft segment (T_{gSS}) of cross-linked PUA was found to be close to the T_g of PEG in the absence of $LiClO_4$. Swelling

Table 1
DSC results of the undoped and $LiClO_4$ doped PUA

Sample	$LiClO_4$ (wt%)	T_{gSS}[a] (°C)	$\Delta T_{gSS}/\Delta C$	T_{gHS}[a] (°C)	T_m[a] (°C)
1	0.0	−52.8	–	–	36.2
2	5.3	−41.7	22.2	52.5	30.8
3	8.8	−34.8	21.6	55.9	–
4	10.6	−29.3	23.4	47.3	–
5	16.0	−20.2	21.7	44.6	–
6	21.0	−12.1	20.3	42.2	–
7	26.6	−3.7	19.6	40.3	–
8	32.0	−0.9	17.3	42.5	–

[a] The results are as available from the instrument with an accuracy of ±0.01°C.

measurements with plasticizer reveal better dimensional stability for the synthesized PUA. Besides that, the presence of acrylate units, –(C(O)–O–C)–, arising from the cross-linking with HEA can alter the conductivity of the doped PUA through interaction with Li^+ ions. A detailed discussion on phase transitions, thermal stability, interaction of soft, hard and HEA groups with Li^+ion and suitability as polymer electrolyte in Li batteries is presented here in the process of evaluating the characteristics of cross-linked PUA as polymer electrolyte.

3.1. Phase transition

Table 1 presents the DSC results of the undoped and $LiClO_4$ doped cross-linked PUA. The parent undoped PUA shows a crystalline endothermic peak appearing at 36°C and a low temperature endothermic transition at −53°C. These two transitions correspond to the melting of the crystalline region (T_m) and the liquid–glass transition of the amorphous region of PEG in the soft segment (T_{gSS}). The additional exothermic peak observed at −33°C is attributed to the recrystallization of the polyether. The T_g of the polyether (PEG-2000) used in this study is −54°C. The measured value of −53°C for the T_{gSS} of the cross-linked PUA is almost equal to that of PEG-2000. Otherwise, there is almost no change in the T_g after reaction with the diisocyanate. Due to the low concentration (27 wt%) of the hard segment and the non-aromatic nature of the hard segment, the change in T_{gSS} is not significant. However, it is relevant to note that TPU prepared with H_{12}MDI and PEG showed an increased T_g (−43.9°C) in comparison with T_g of PEG [22]. It may also be viewed that PEG-2000 is long enough to make the changes in T_g as it is insensitive to the nature of chain ends. Hence, the closeness of T_{gSS} of cross-linked PUA with T_g of PEG signifies that the cross-linking induced by HEA provides less influence on the flexibility of soft segment, –(O–CH_2–CH_2)–.

In the presence of $LiClO_4$, the crystalline structure of PEG in doped PUA is disrupted as evident from the absence of peak corresponding to crystalline region. This informs that doped PUA is transformed into amorphous with the addition of $LiClO_4$. As can be seen from Table 1, the melting transition is vanished after addition of >5.3 wt% of $LiClO_4$. For all the doped samples, one high temperature (~40–50°C) endothermic transition has been observed, which is due to the hard segment T_g (T_{gHS}). T_{gHS} is not observed for the undoped sample. The very high endothermic melting transition might have obscured the high temperature transition of the undoped sample. The transition temperatures for all these events are observed to change with increase in $LiClO_4$ concentration. Several authors have studied the thermal behavior of TPU by DSC [11,27,28]. Leung et al. [27] reported the increase in T_{gSS} from near −80 up to 30°C when the TPU hard segment content is increased to 80%. They also observed that T_{gHS} is around 100°C for TPU containing more than 30 wt% hard segment. But the TPU systems with less than 30 wt% hard segment are reported [11,28–30] as not having such high temperature (>100°C) endotherms. Such is the case for the cross-linked PUA which contains 27 wt% of hard segment and hence does not show any high temperature (>100°C) transition.

The variation of both hard and soft segment T_g with salt concentration is shown in Fig. 2. From Fig. 2 and Table 1, it is inferred that incorporation of salt into the polymer matrix leads to an increase in T_{gSS}. This is consistent with the previous reports [11–22] of $LiClO_4$-doped TPUs containing PEO, PPO or PTMO as the soft segment and of polyether complexes with $LiCF_3SO_3$, [27] where an increase in T_g with salt concentration is observed. Increase in T_{gSS} with salt concentration indicates stiffening of the polyether chain due to ion dipole interaction between the Li^+ ions and the polyether oxygens. Table 1 also contains the $\Delta T_g/\Delta C$ values, which are obtained by normalizing the T_g data with respect to the concentration of $LiClO_4$. The $\Delta T_g/\Delta C$ values reaches a maximum at ~10.6 wt% of $LiClO_4$ and thereafter shows a decreasing trend. The decreasing trend indicates the predominant charge-neutral contact ion pair formation at concentration beyond 0.6 wt% $LiClO_4$ (Table 1 and Fig. 2). Interestingly, ^{7}Li NMR spectroscopic analysis and AC impedance measurements also predict ion pair formation beyond 10.6 wt% of $LiClO_4$ (discussed later). A decreasing

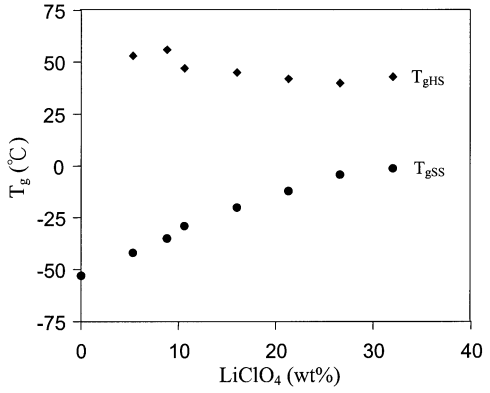

Fig. 2. Variation of soft segment and hard segment T_g of PUA with salt concentration.

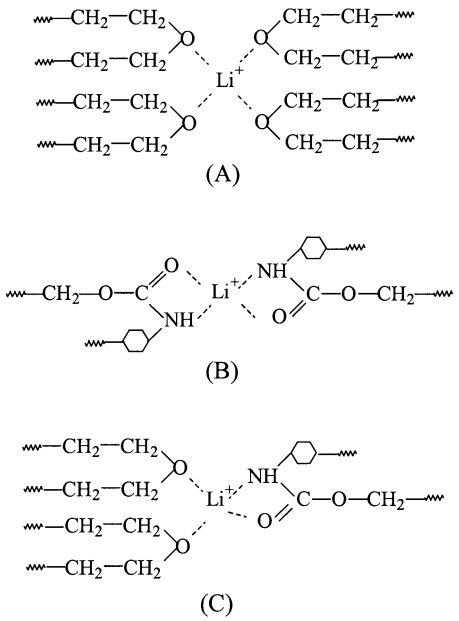

Fig. 3. Schematic representation of different complexes formed by the interaction of Li^+ with: (A) polyether chains, (B) –NH and C=O groups of urethane links, and (C) both ether and urethane groups.

trend in T_{gHS} was noticed with increase in salt concentration. The phase mixing of hard and soft segments in PUA in the presence of $LiClO_4$ may be the reason for such a trend. This results also in simultaneous increase in T_{gSS}. The variation of hard and soft segment T_g values with salt concentration can be explained further on the basis of various types of interactions of groups present in PUA with the Li^+ ions, as mentioned below.

Due to the presence of different coordination sites in the PUA system, various types of complexes can be formed by the interaction of these coordination sites with the Li^+ ions. Three major types of interactions can be distinguished [22]: (1) interaction of the ether oxygens with the Li^+ ions, as mentioned earlier, leading to the formation of transient cross-links between the polyether chains via the Li^+ ions, which restricts the segmental motion, (2) interaction of urethane –NH and carbonyl groups with the Li^+ ions leading to inter or intra molecular cross-linking, and (3) mixed ether–urethane interactions with the Li^+ ions leading to phase mixing of the hard and soft segments. Three types of complexes arising out of the above three interactions are shown schematically in Fig. 3. Formation of such complexes has earlier been reported for composite systems like PEO–poly(vinyl pyridine)–$LiClO_4$ [30] and PEO–poly(*N*,*N*-dimethyl acrylamide)–$LiClO_4$ [31]. Besides that, the oxygen present in the acrylate group may also coordinate with Li^+ ions. This possibility was further explored by FTIR spectroscopic analysis.

3.2. Ion–polymer interaction

The effect of salt concentration on the interaction of Li^+ ions with groups in PUA has been investigated by FTIR spectroscopy. In order to gain insight into the effect of Li^+ ions on the H-bonding interactions of the hard and soft segments, three regions of the FTIR spectrum have been chosen: (1) 3800–3100 cm^{-1}, the region for free and H-bonded –NH stretching mode, (2) 1750–1650 cm^{-1}, the region for urethane carbonyl symmetric stretching vibration, and (3) 1200–1100 cm^{-1}, the region for C–O–C stretch of PEG, C(O)–O–C stretch of the hard segment and C(O)–O–C– stretch of acrylate group.

Table 2
Deconvolution results of the FTIR spectra in the –NH stretching region

Sample	$LiClO_4$ (wt%)	Peak positions (cm^{-1})			Percent area		
		1	2	3	1	2	3
1	0.0	3556	3453	3331	35.2	8.9	55.9
2	5.3	3550	3399	3245	24.1	66.2	9.7
3	10.6	3548	3407	3248	22.3	67.1	10.6
4	21.0	3564	3426	3251	17.0	65.9	17.1

3800–3100 cm^{-1} *region*. The –NH stretching region of the FTIR spectra is characterized by three modes of vibrations [32]. The deconvoluted spectra of the undoped and three of the doped samples are presented in Fig. 4 and the results are given in Table 2. As shown in Fig. 4, the peak in the region of 3572–3548 cm^{-1} is due to the free –NH stretching vibration. The other two peaks in the regions of 3450–3400 and 3330–3245 cm^{-1} are assigned to the

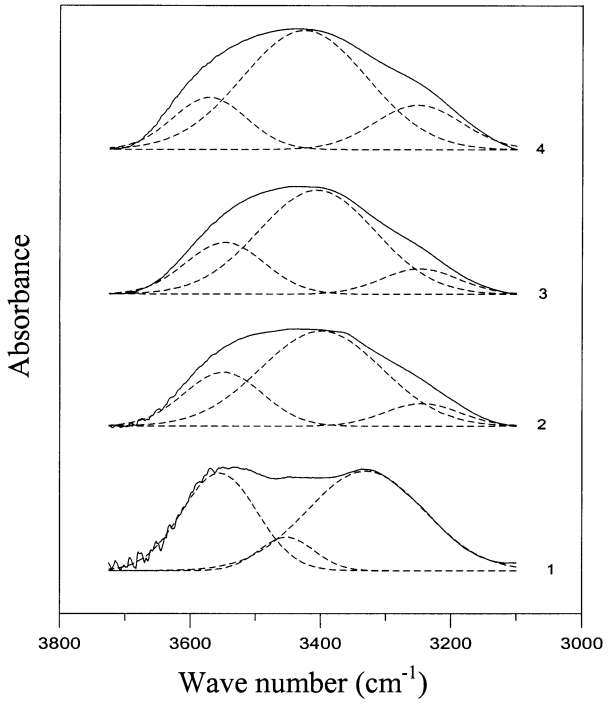

Fig. 4. Deconvolution of the –NH stretching mode of PUA containing different amount of $LiClO_4$: (1) 0.0 wt%, (2) 5.3 wt%, (3) 10.6 wt%, (4) 21.0 wt%.

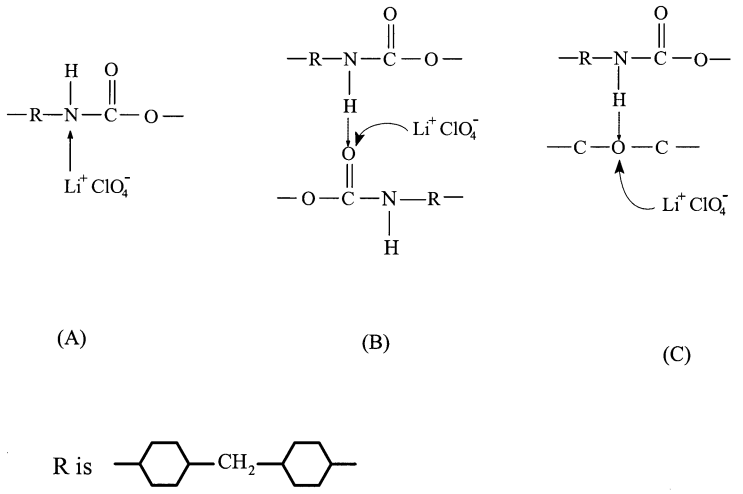

Fig. 5. Schemetic representation of coordination of Li^+ ions to different positions: (A) to the nitrogen atoms of free –NH groups, (B) to the hydrogen bonded carbonyl oxygens, and (C) to the hydrogen bonded ether oxygens.

H-bonded –NH stretching, where the H-bonding is formed with the carbonyl and the ether oxygens, respectively [32,33]. An examination of Table 2 indicates that all the three peaks undergo shifting towards lower frequency when doped with $LiClO_4$. The shifting of the peak positions is due to the possible interactions of Li^+ ions with the different coordination sites of PUA, as schematically shown in Fig. 5. The shifting of the free –NH band position to the lower frequency in the presence of $LiClO_4$ may be attributed to the coordination of Li^+ ions to the nitrogen atoms of the free –NH groups (Scheme A, Fig. 5). The two H-bonded peaks are also found to be shifted towards lower frequency after addition of $LiClO_4$. Shifting of the H-bonded –NH band positions to lower frequency can be explained with the help of Schemes B and C (Fig. 5).

Table 2 also shows the respective peak areas for all the –NH bands. The peak areas are normalized against the total –NH band area. As the absorptivity coefficient of –NH groups in a TPU is reported [34,35] to be a strong function of strength of the H-bonds and band frequency, quantitative measurement of the free and H-bonded –NH groups is not possible from the peak area values. However, a qualitative idea can be generated on the relative extent of interaction of Li^+ ions with the hard and soft segments [36]. It is evident from the area values that the extent of –NH groups H-bonded to the ether oxygens is more in the absence of Li-salt. But in presence of Li-salt, the –NH groups H-bonded to the carbonyl oxygens become higher. This is quite reasonable in the sense that, with the addition of salt, the Li^+ ions preferentially coordinate to the easily accessible ether groups and hence reduced the extent of –NH groups which are H-bonded to the ether oxygens.

1750–1650 cm^{-1} region. The deconvoluted FTIR spectra of the undoped and the doped samples are used to obtain the percent areas (Table 3) for the carbonyl stretching vibrations: the free or non-H-bonded C=O (1730–1722 cm^{-1}) and two stretching vibrations associated with disordered (1719–1711 cm^{-1}) and ordered (1703–1696 cm^{-1}) H-bonded C=O [15]. The three peaks are shifted to lower frequency by the addition of Li-salt. This may be attributed to the coordination of electron deficient Li^+ ions with the carbonyl oxygen atoms, which weakens the C=O bond by sharing the electron density of the carbonyl oxygen atoms.

1200–1000 cm^{-1} region. The deconvoluted FTIR spectra of the undoped and doped PUA samples represent four characteristic vibrational modes (Table 4) and the associated areas: (1) the peak in the region of 1146–1145 cm^{-1} region is assigned to the C(O)–O–C stretch of the acrylate groups [36], (2) the second peak in the region of 1111–1106 cm^{-1} region is assigned to the C–O–C stretch of PEG, (3) the peak in the region of 1088–1074 cm^{-1} is due to the C(O)–O–C stretch of the urethane groups, and (4) the fourth one in the region of 1042–1035 cm^{-1} is assigned to the H-bonded C–O–C stretch of PEG [15]. The data from Table 4, clearly demonstrates that the acrylate C(O)–O–C stretch does not show any change in its band position by the addition of Li-salt. Both the C(O)–O–C stretch of the urethane groups and the C–O–C stretches show a shift to lower frequency with the addition of Li-salt. This is consistent with the earlier observations [15] of a MDI/PTMO/BDO based TPU system. A comparison of the percent area reveals that upon adding the salt some of the H-bonded C–O–C groups become free. This may be due to the interaction of Li^+ ions

Table 3
Deconvolution results of the FTIR spectra in the C=O stretching region

Sample	$LiClO_4$ (wt%)	Peak positions (cm^{-1})			Percent area		
		1	2	3	1	2	3
1	0.0	1729	1719	1703	8.1	46.9	45.0
2	5.3	1730	1719	1701	5.1	45.5	49.4
3	10.6	1722	1711	1696	25.3	43.5	31.2
4	21.0	1727	1716	1700	12.0	39.2	48.8

Table 4
Deconvolution results of the FTIR spectra in the ether-stretching region

Sample	$LiClO_4$ (wt%)	Peak positions (cm^{-1})				Percent area			
		1	2	3	4	1	2	3	4
1	0.0	1146	1114	1091	1042	13.5	52.7	28.0	5.8
2	5.3	1145	1110	1083	1039	7.4	58.4	29.6	4.6
3	10.6	1145	1108	1078	1038	5.1	67.8	23.0	4.1
4	21.0	1146	1110	1073	1035	6.8	55.8	34.2	3.2

with the ether oxygens leading to a decrease in the electron density of the ether oxygens and its ability to form H-bond. All these observations indicate that introduction of Li-salt into PUA results in various types of interactions leading to a change in the microstructure of the polymer. The formation of a new microstructure, due to these interactions, is also evident from our other experiments such as TGA and NMR.

3.3. Thermal stability

Typical TG curves for the undoped and doped PUA systems are shown in Fig. 6. As can be seen from Fig. 6, the pure polymer decomposes in a single step beginning at 394°C. The introduction of the salt promotes the decomposition of the PUA. The decreasing trend in the initial decomposition temperature (T_d) for the samples with increasing $LiClO_4$ concentration (up to 10.3 wt% of $LiClO_4$) is shown in the inset of Fig. 6. This behavior may be explained on the basis of weakening of the C–O bond, caused by the decrease in electron density due to the interaction of Li^+ ions with the oxygen atoms. Alternatively, perchlorate oxidation of PEO phase can cause this thermal event starting from ~380°C. The observed trend in thermal transitions at higher $LiClO_4$ concentrations (beyond 10.3 wt% of $LiClO_4$) may arise from the predominant perchlorate oxidation.

3.4. ^7Li MAS NMR spectroscopy

^7Li MAS NMR was used to acquire further evidence on the interaction of Li^+ ions with PUA, which results in the creation of a new microstructure. It has been found from our earlier communication [21] that the NMR line widths decrease significantly as the proton decoupling was applied on acquiring the ^7Li MAS NMR spectra. This implies that there are significant ^7Li–^1H dipolar interactions of lithium cations and polymer backbone. Fig. 7 shows the variable temperature ^7Li proton decoupled MAS NMR spectra of the PUA doped with 10.6 wt% $LiClO_4$. It is evident from Fig. 7 that more than one resonance due to the presence of various local environments of Li^+ ions become well resolved at lower temperature. On raising the temperature, the three resonances begin to shift and eventually merge into a single resonance. As will be discussed later, there are three resonance sites (I, II, and III, Fig. 8), assigned to the Li^+ ions coordinated to the urethane groups, ether groups and those are in the form of ion pairs/aggregates, respectively. As the number of free ions (and hence the ion pairs) is dependent

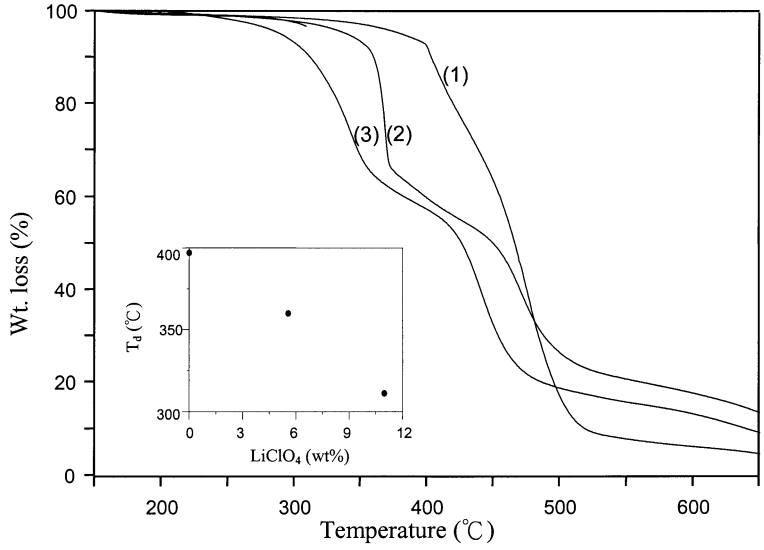

Fig. 6. Typical TG curves of PUA containing different amount of $LiClO_4$: (1) 0.0 wt%, (2) 5.3 wt%, (3) 10.6 wt%, (4) 21.0 wt%. Inset: variation of T_d with $LiClO_4$ concentration.

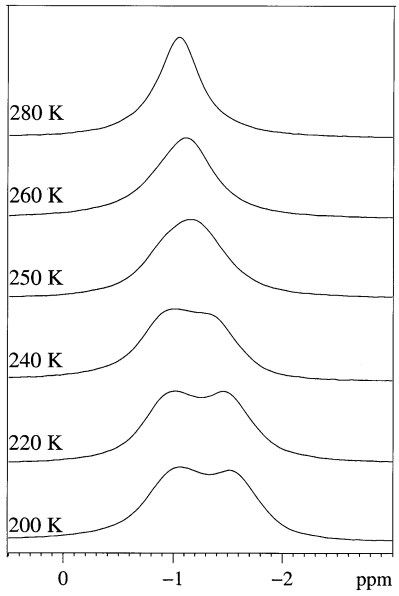

Fig. 7. Variable-temperature proton-decoupled ^{7}Li MAS NMR spectra of a PUA doped with 10.6 wt% $LiClO_4$.

on temperature [15], site III may disappear at higher temperature leading to an increase in the intensity of sites I and II. In addition, there is a classical peak merging of sites I and II at higher temperature, by a two-site exchange process. However, a temperature dependent site preference may also exist [37] in addition to the two-site exchange process. At lower temperature, the frequency of the exchange process must be greater than the separation of the resonances for an effective exchange to occur. At higher temperature, cation exchange is faster than the NMR time scale, which results in a single resonance with a chemical shift that is a weighted average of the individual components.

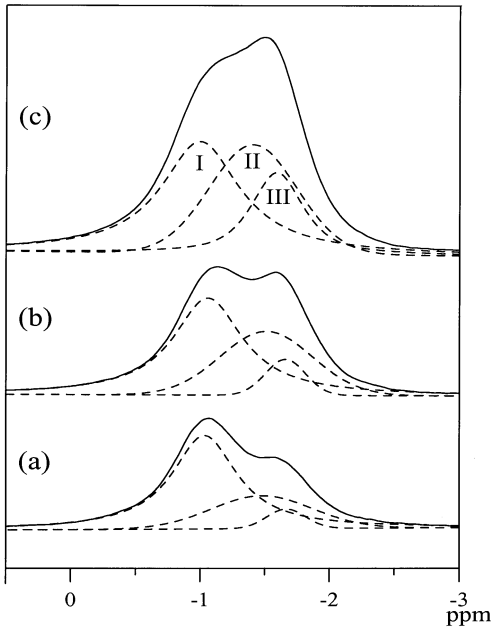

Fig. 8. Deconvolution of proton-decoupled ^{7}Li MAS NMR spectra at 200 K for PUA samples doped with (a) 5.3 wt%, (b) 10.6 wt%, and (c) 21.0 wt% $LiClO_4$.

It is to be mentioned that the temperature at which the individual resonances merge into a single one is dependent on the salt concentration. It was found to increase with the increase in salt concentration. For the sample containing 5.3 wt% $LiClO_4$, this temperature is ~240 K, whereas for the samples containing 10.6 and 21.0 wt% $LiClO_4$, it is ~250 and ~270 K, respectively. This indicates that with the increase in salt concentration the exchange process becomes slower at a particular temperature. This may be due to the increase in T_g of the polymer with the increase in salt concentration. Increase in T_g leads to a decrease in free volume at a given temperature and, hence, lower ionic mobility.

Fig. 8 presents the ^{7}Li NMR spectra as a function of salt concentration recorded at 200 K. Deconvolution of the NMR spectra shows a mixture of Lorentzian/Gaussian lines for all the three resonances. The three doped samples exhibit three characteristic sites in the regions of −1.03 (site I), −1.45 (site II), and −1.60 (site III) ppm. On the basis of our earlier communication [21] site I is assigned to the Li^+ ions coordinated to the urethane groups of the hard segment, whereas site II is associated to the Li^+ ions coordinated to the ether oxygens of the soft segment. The observation of site III in the lower frequency region is attributed to the Li^+ ions in the form of ion pairs or aggregates. It is to be noted that the intensity of site III is increased with the increase in salt concentration, when the intensity of site I is normalized. The intensity of site II (normalized against site I) shows an increasing trend up to 10.6 wt% salt concentration. Beyond that, it is almost constant. This indicates that with the increase in salt concentration beyond 10.6 wt%, there is only a proportional increase in the Li^+ ions in the soft segment. More and more Li^+ ions are residing in site III as ion pairs. These observations are consistent with the DSC results which shows a maximum for $\Delta T_g/\Delta C$ at 10.6% of $LiClO_4$. It is pertinent to note that our conductivity data also shows a maximum conductivity in the same range (10–12 wt% of $LiClO_4$) of salt concentration (discussed later). On the basis of the fact that conductivity mainly results from the Li^+ ions in the soft segment of TPU electrolytes, the above observations made in NMR and conductivity measurements are quite reasonable and consistent.

3.5. Ionic conductivity

The ionic conductivity data obtained from AC impedance measurements as a function of $LiClO_4$ concentration at 25°C is shown in Fig. 9. The system shows an increase in conductivity with salt concentration and a maximum is observed in the salt concentration range of 10–12 wt% of $LiClO_4$ with a maximum conductivity of the order of 1×10^{-6} S cm^{-1} at 25°C. This is almost similar to the maximum conductivity

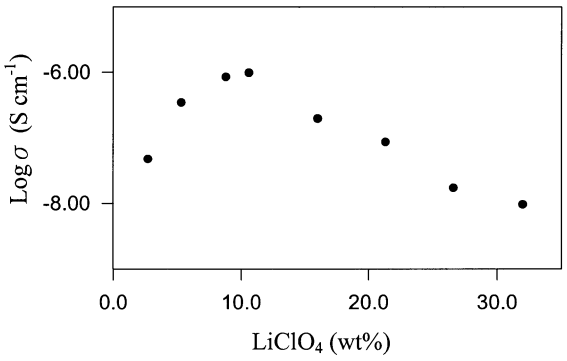

Fig. 9. Variation of conductivity of PUA electrolytes with $LiClO_4$ concentration at 25°C.

reported by Furtado et al. [20] for a hexamethylene diisocyanate/PTMG/PEG based TPU having 17 wt% hard segment. The conductivity generally increases with salt concentration by an order or two [38]. Following the maximum, the conductivity decreases for higher salt concentration. This feature is the reflection of two opposite effects, namely the increase in the number of charge carriers [39] and decrease in the free volume [40,41]. As the concentration of salt is increased, the number of charge carriers is also increased, but the average free volume is decreased due to the increase in T_g (as a result of the interaction of Li^+ with the ether oxygens). At low concentration of salt, the increase in the number of charge carriers dominates, whereas at high salt concentration level, the reduction of free-volume takes precedence [42]. When the salt concentration reaches ~12 wt% or more, the decrease in free-volume becomes more pronounced than the increase in number of charge carriers. At this stage, the lower fraction of free volume is no longer compensated by the continuous increase in the number of charge carriers. As a result of which, conductivity is decreased with an increase in salt concentration at higher salt concentration level. Additionally, at higher salt concentration considerable amount of salt remains as ion-pairs, which do not contribute to the conductivity of the electrolyte.

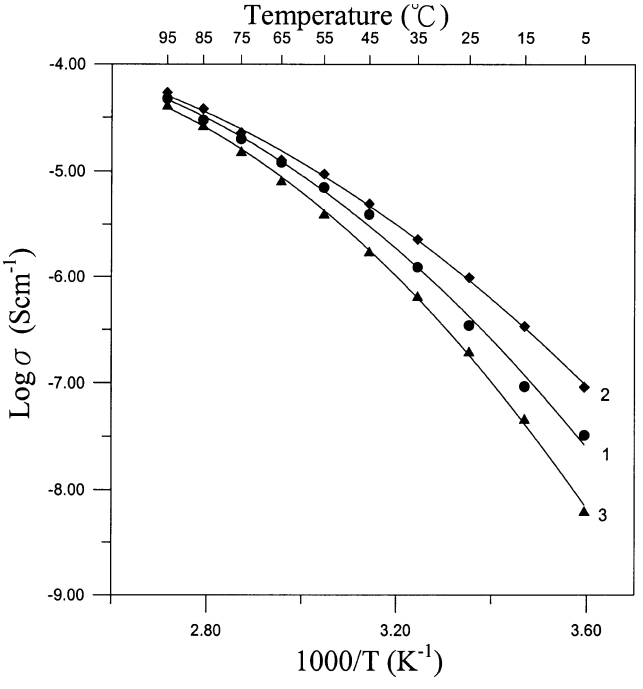

Fig. 10. Temperature dependence of ionic conductivity of PUA doped with different amount of $LiClO_4$ (1) 5.3 wt%, (2) 10.6 wt%, (3) 16.0 wt%.

3.5.1. Temperature dependence of conductivity

Fig. 10 shows the temperature dependence of ionic conductivity of some of the PUA/$LiClO_4$ complexes. From this figure it is evident that the temperature dependence of conductivity is not linear, which is in line with the observations made by other researchers [14,15]. The non-linear dependence of conductivity with temperature can be best explained with the help of Vogel–Tamman–Fulcher (VTF) relationship, where the transport of charge carriers is considered to be coupled with the segmental motion of the polymer host.

$$\sigma(T) = AT^{-1/2}\exp[-B/k_B(T - T_0)] \quad (4)$$

where $\sigma(T)$ is the conductivity at temperature T, A is a constant proportional to the number of charge carriers, B is the pseudoactivation energy related to the polymer segmental motion, k_B is the Boltzmann constant and T_0 is the reference temperature at which the configurational entropy of the polymer becomes zero and is close to the glass transition temperature.

It is evident from Fig. 10 that the conductivity of sample 2 is the highest among the three (also shown in Fig. 9) throughout the temperature range. It is known that ionic mobility is constant at a given $T - T_g$, iso-volume state, and the ionic conductivity increases with increase in the number of charge carriers [43–45]. The comparison of log σ with $T - T_g$ is shown in Fig. 11. An examination of Fig. 11 indicates that sample 3 shows higher conductivity than sample 1, which was otherwise reverse (see Fig. 10), when contribution from both the factors were considered. But it is still lower than sample 2. Since, the higher conductivity of sample 3 (compared to sample 1) is due to higher number of charge carriers at higher salt concentration. But the reason for its having lower value compared to sample 2 is ascribed to the increased ion pair formation with the increase in salt concentration. This observation is consistent with the results from DSC (Table 1) and ^7Li NMR spectroscopic studies. However, at higher temperature both the samples show similar conductivity in the iso-free-volume condition as the number of charge carriers is expected to be temperature-dependent. With increase in temperature, some of the ion pairs undergo dissociation leading to an increase in the number of free ions.

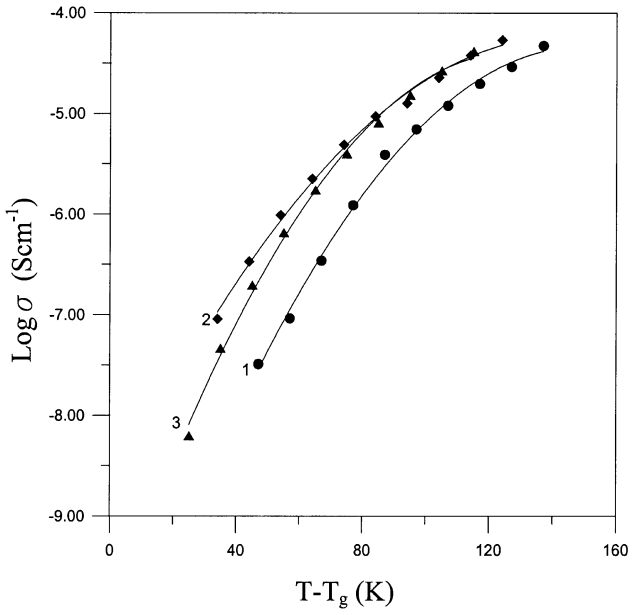

Fig. 11. Relation between $(T - T_g)$ and the ionic conductivity of PUA doped with different amount of $LiClO_4$ (1) 5.3 wt%, (2) 10.6 wt%, (3) 16.0 wt%.

3.6. Suitability of cross-linked PUA as polymer electrolyte

In order to check the stability of the cross-linked films in liquid electrolytes, the polymer films were allowed to swell in two commercial battery electrolytes (LP-20 and LP-30) for different time periods. It has been found that the cross-linked PUA is very much stable in both the liquid electrolytes, even after swelling of ~250 wt%. The mechanical property of the films is good enough for use as electrolyte material. Ionic conductivity of the order $\sim 10^{-3}$ S cm^{-1} has been obtained for a 250 wt% swelled film at room temperature. Comparable ionic conductivity of these cross-linked electrolytes to PEO combined with the very good dimensional stability is expected to make the cross-linked PUA as a potential candidate for use as battery electrolyte.

Acknowledgements

The financial support of this work by the National Science Council of Taiwan under NSC 88-2622-E006-008 and NSC 89-2214-E006-012 is gratefully acknowledged. The authors wish to thank Prof. H.M. Kao of National Central University, Chung Li and Ms Ru-Rong Wu of the NMR laboratory for their help with the NMR experiments.

References

[1] MacCallum JR, Vincent CA, editors. Polymer electrolyte reviews Polymer electrolyte reviews, vols. 1 and 2. London: Elsevier, 1987/1989.
[2] Gray FM. Solid polymer electrolytes — fundamental and technological applications. Weinheim, Germany: VCH, 1991.
[3] Scrosati B. Application of electroactive polymers. London: Chapman & Hall, 1993.
[4] Ratner M. In: MacCallum JR, Vincent CA, editors. Polymer electrolyte reviews, vol. 1. London: Elsevier, 1987. Chapter 1.
[5] Berthier C, Gorecki W, Minier M, Armand MB, Chabagno JM, Rigaud P. Solid State Ionics 1983;11:91.
[6] Blonsky PM, Shriver DF, Austin P, Allcock HR. J Am Chem Soc 1984;106:6854.
[7] Blonsky PM, Shriver DF, Austin P, Allcock HR. Solid State Ionics 1986;18/19:258.
[8] Tonge JS, Shriver DF. J Electrochem Soc 1987;134:269.
[9] Bennett JL, Dembek AA, Allcock HR, Heyen BJ, Shriver DF. Chem Mater 1989;1:14.
[10] LeNest JF, Gandini A, Cheradame H. Br Polym J 1986;20:253.
[11] McLennaghan AW, Pethrick RA. Eur Polym J 1988;24:1063.
[12] McLennaghan AW, Hooper A, Pethrick RA. Eur Polym J 1989;25:1297.
[13] Watanabe M, Oohashi S, Sanui K, Kobayashi T, Ohtaki Z. Macromolecules 1985;18:1945.
[14] Watanabe M, Sanui K, Ogata N. Macromolecules 1986;19:815.
[15] van Heumen JD, Stevens JR. Macromolecules 1995;28:4268.
[16] Seki M, Sato K. Makromol Chem 1992;193:2971.
[17] Forsyth M, Macfarlane DR, Meakin P, Smith ME, Bustow TJ. Electrochim Acta 1995;40:2343.
[18] Ferry A, Jacobson P, van Heumen JD, Stevens JR. Polymer 1996;37:737.
[19] Ng STC, Forsyth M, Macfarlane DR, Garcia M, Smith ME, Strange JH. Polymer 1998;39:6261.
[20] Furtado C, Silva GG, Machado JC, Pimenta MA, Silva RA. J Phys Chem B 1999;103:7102.
[21] Wang HL, Kao HM, Wen TC. Macromolecules 2000;33:6910.
[22] Wang HL, Kao HM, Digar ML, Wen TC. Macromolecules 2001;34:529.
[23] Cooper SL, Tobolsky AV. J Appl Polym Sci 1967;11:1361.
[24] Mocanin J, Cuddihy EF. J Polym Sci C 1966;14:313.
[25] Santaniello E, Manzocchi A, Sozzani P. Tetrahedron Lett 1979;47:4581.
[26] Armand MB, Chabagno JM, Duclot MJ. In: Vashishta P, Mundy JN, Shenoy GK, editors. Fast ion transport in solids. New York: Elsevier, North-Holland, 1979. p. 131.
[27] Leung L, Koberstein J. Macromolecules 1986;19:706.
[28] Seymour R, Cooper SL. Macromolecules 1973;6:48.
[29] Albinson I, Mellander BE, Stevens JR. J Chem Phys 1992;96:681.
[30] Li J, Khan IM. Macromolecules 1993;26:4544.
[31] Wieczorek W, Zalewska A, Raducha D, Florjanczyk Z, Stevens JR, Ferry A, Jacobson P. Macromolecules 1996;29:143.
[32] Solomon M, Xu M, Eyring EM, Petrucci SJ. Phys Chem 1994;98:8234.
[33] Lee HS, Wang YK, Hsu SL. Macromolecules 1987;20:2089.
[34] Coleman MM, Lee KH, Skrovanek DJ, Painter PC. Macromolecules 1986;19:2149.
[35] Coleman MM, Skrovanek DJ, Painter PC. Macromolecules 1985;18:299.
[36] Pouchert CJ, editor. The Aldrich Library of infra-red spectra, 1978.
[37] Abragam A. The principle of nuclear magnetism. Oxford: Oxford University Press, 1961.
[38] Robitaille CD, Fauteux DJ. J Electrochem Soc 1986;133:315.
[39] Ferry A, Oradd G, Jacobson P. J Chem Phys 1998;108:7426.
[40] Cohen MH, Turnbull D. J Chem Phys 1959;31:1164.
[41] Gray FM. Polymer electrolytes. In: Connor JA, editor. RSC materials monograph, 1st ed. The Royal Society of Chemistry, London, 1997.
[42] Peng ZL, Wang B, Li SQ, Wang SJ, Liu H, Xie HQ. Phys Lett A 1994;194:228.
[43] Peng X, Wu S, Chen D. Solid State Ionics 1993;59:197.
[44] Hu CP, Wright PV. Br Polym J 1989;21:421.
[45] Killis A, LeNest JF, Cheradame H, Gandini A. Makromol Chem 1982;193:2836.